And., Intl.,J., Appl Sci., Eng., Tech, Vol 05, No 03, November 2025
e-ISSN: 2797-0442

Comparison of Seismic Performance of Shear Wall and Bracing Systems in Residential Flats in Silangkitang Village North Tapanuli

Muhammad Fauzan Abiyyu*, Samsul Abdul Rahman Sidik Hasibuan
Department of Civil Engineering, Faculty of Engineering, Medan Area University, Indonesia
*Corresponding author, e-mail: fauzanabiyyu2001@gmail.com

Abstract—Indonesia lies within the Pacific Ring of Fire at the convergence of three major tectonic plates, making earthquake-resistant design a critical challenge for multi-story buildings. Structural systems such as reinforced concrete shear walls and steel bracing are commonly employed to enhance lateral load resistance. This study evaluates and compares the seismic performance of shear wall and bracing systems in a three-story residential flat located in Silangkitang Village, North Tapanuli, using nonlinear static (pushover) analysis conducted in ETABS v18. The analysis results indicate that, in the X-direction, the shear wall structure achieves a total displacement of 66.84 mm with a base shear of 8512.78 kN, whereas the braced structure exhibits a total displacement of 119.19 mm with a base shear of 9773.20 kN. In the Y-direction, the shear wall structure records a total displacement of 166 mm and a base shear of 13,228.69 kN, while the braced structure achieves 173 mm and 8210.53 kN, respectively. These findings demonstrate that, although both systems satisfy the same structural performance level criteria, the shear wall system provides superior lateral stiffness and more favorable displacement characteristics compared to the bracing system.

Keywords: Nonlinear pushover, Shear wall, Bracing, Displacement, and Base shear.

This article *is licensed under the CC–BY-SA license.*

1. Introduction

Indonesia is geographically located at the convergence of the Indo-Australian, Eurasian, and Pacific tectonic plates, within the Pacific Ring of Fire [1], [2]. This geodynamic setting exposes the region to frequent and potentially devastating seismic events, posing significant challenges in the design and construction of earthquake-resistant multi-story buildings [3]–[5]. The structural integrity of such buildings must be capable of resisting both gravity and lateral loads, particularly those induced by wind and seismic actions [6]–[8].

To improve seismic performance, engineers commonly integrate lateral force-resisting systems such as reinforced concrete (RC) shear walls or steel bracing [9]–[12]. While both systems enhance structural stiffness and strength, their mechanical behavior and contribution to seismic resistance differ. RC shear walls act as vertical cantilever elements that primarily resist shear forces generated by seismic excitation. Ideally, damage in shear walls is controlled by flexural yielding through the formation of plastic hinges at the wall base, rather than by brittle shear failure [13]–[16]. In contrast, bracing systems consist of concentric or eccentric diagonal members that transfer lateral loads into axial forces within the frame, providing an efficient yet mechanically distinct seismic load path [17], [18].

Evaluating the seismic performance of buildings employing these systems can be performed using either elastic or nonlinear analysis. Nonlinear static (pushover) analysis has become a widely adopted method for performance-based seismic evaluation, as it captures the inelastic response of a structure under incrementally increasing lateral loads until significant yielding or collapse mechanisms are observed [19]–[21]. The structural performance level is then determined by quantifying damage states and relating them to functional criteria, commonly classified as Immediate Occupancy (IO), Damage Control (DC), Life Safety (LS), and Structural Stability (SS) [22], [23]. These performance levels are

Received: October 13, 2024, Revised: August 31, 2025, Accepted: October 3, 2025
https://doi.org/10.25077/aijaset.v5i3.191

typically evaluated by comparing the maximum interstory drift to predefined acceptance criteria derived from the capacity curve, as shown in Figure 1, and summarized in Table 1 [24], [25].

Figure 1 presents the effective fundamental parameters of a typical capacity curve, which represent the nonlinear relationship between lateral load and displacement. Table 1 lists the drift-based parameters used for performance evaluation, including the maximum total drift and inelastic drift ratio thresholds associated with each structural performance level.

For pushover analysis, lateral loads are applied following specific patterns to simulate seismic effects. In addition to gravity loads, at least 25% of the design live load is combined with the dead load, and lateral loads are applied to the center of mass at each story. According to FEMA recommendations, at least two distinct lateral load distributions should be considered to capture the worst-case response scenarios, typically applied monotonically in one principal direction.

Given the increasing demand for cost-effective and seismically resilient housing infrastructure in seismically active regions such as North Sumatra, it is essential to evaluate and optimize lateral force-resisting systems. Although shear walls and bracing systems are widely used, comparative studies focusing on their seismic performance in low- to mid-rise residential flats remain limited. This research addresses that gap by performing a nonlinear static (pushover) analysis to assess and compare the structural performance of buildings utilizing shear walls and bracing systems. The novelty of this study lies in providing a direct performance-based comparison of these two structural systems under the same architectural and loading conditions, applied to a real-world residential flat project in Silangkitang Village, Sipoholon District, North Tapanuli Regency.

Accordingly, the objectives of this study are: (1) to evaluate the nonlinear seismic response of shear wall and bracing systems in a three-story residential flat, (2) to compare their lateral stiffness, displacement demand, base shear capacity, and plastic hinge distribution, and (3) to determine the performance level of each system in accordance with performance-based seismic design criteria. The findings are expected to inform structural engineers and decision-makers in selecting optimal lateral force-resisting systems for similar building types in earthquake-prone regions.

Table 1. Parameters for performance evaluation on building structures

Parameter	**Performance level**			
	IO	**Damage control**	**LS**	**Structural Stability**
Maximum total drift	0.01	0.01 – 0.02	0.02	$0.33\frac{\text{Vi}}{\text{Pi}}$
Maximum Inelastic drift ratio	0.005	0.005 – 0.015	Not limited	Not limited

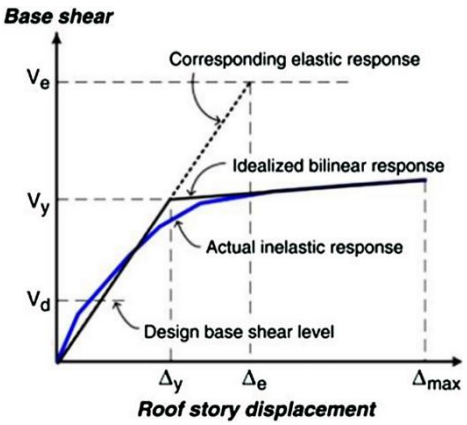


Figure 1. Effective Fundamental Parameters of the Capacity Curve

2. Method

This research employs a nonlinear static (pushover) analysis using ETABS v18 to evaluate the seismic performance of two residential flat models: one incorporating shear walls and the other using bracing systems. The methodology consists of four primary stages: data collection, structural modeling, load assignment, and performance assessment [26].

2.1 Data Collection and Structural Modeling

The required data include architectural shop drawings and geotechnical soil reports, which serve as the basis for accurate structural modeling [27], [28]. The case study building is a three-story reinforced concrete residential flat located in Silangkitang Village, Sipoholon District, North Tapanuli Regency. The total building height is 14,600 mm. The geographic location of the project site is illustrated in Figure 2, while the current construction condition is shown in Figure 3.

The building was modeled in ETABS v18 according to national standards [29]. The seismic design parameters indicate that the site falls within Earthquake Risk Category II and is situated on soft soil (Site Class SE) [30]. Operational loads were assigned based on its function as an apartment/flat [31]. The structural system includes two reinforced concrete shear walls — shear wall 1 with a net length of 1680 mm and shear wall 2 with a net length of 3550 mm. For the alternative bracing system, steel Wide Flange (WF) 300 × 150 profiles were used. The selection of this steel section considered the installation cost relative to the shear wall system, with minimal price differences, as later detailed in Tables 2 and 3 [32], [33].

2.2 Load Patterns and Pushover Analysis Procedure

Gravity loads consist of dead loads combined with 25% of the design live loads, as recommended for pushover analysis [34]. Lateral loads are applied incrementally at the center of mass of each story. According to FEMA guidelines [35], at least two lateral load patterns must be considered to capture the worst-case structural response. The loads are applied monotonically in both the X- and Y-directions until plastic hinge formation and global instability are observed [36].

The pushover analysis produces capacity curves representing base shear versus roof displacement, from which key response parameters — such as ultimate base shear capacity, maximum lateral displacement, and plastic hinge distribution — are extracted for both structural systems [37].

2.3 Structural Performance Criteria and Calculation

To evaluate the performance level of the structures, maximum drift ratios are calculated by dividing the total lateral displacement by the building height, as expressed in Equation (1):

$$\Delta_{\max drift} = \frac{\Delta_{roof}}{H_{building}} \tag{1}$$

Where Δ_{roof} is the maximum roof displacement (mm), and $H_{building}$ is the total building height (mm).

The computed drift ratios are compared with performance thresholds corresponding to Immediate Occupancy (IO), Damage Control (DC), Life Safety (LS), and Structural Stability (SS). The drift-based acceptance criteria, adopted from ATC-40 and FEMA 440 guidelines, are summarized in Table 1 (presented in the Introduction). These criteria allow classification of each structural system's seismic performance level, enabling engineers to determine whether the structure remains functional, requires repair, or risks collapse under different seismic hazard levels.

Additionally, the story shear distribution and interstory drift profiles are extracted from ETABS outputs. These parameters are analyzed to assess not only global building performance but also floor-by-floor behavior, including the identification of soft-story mechanisms or irregularities that may lead to localized failures. Furthermore, the correlation between base shear capacity and displacement demand is examined to evaluate whether the lateral force-resisting system provides sufficient stiffness, ductility, and energy dissipation capacity to achieve the intended performance objectives in line with modern seismic design principles.

AIJASET – Vol. 05, No. 03, November 2025. 251-263
https://doi.org/10.25077/aijaset.v5i3.191

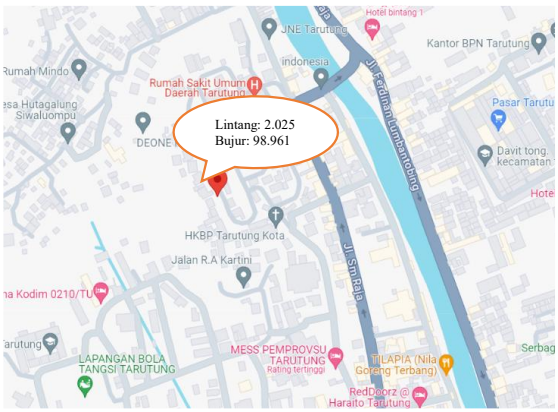


Figure 2. Location of Silangkitang Village Flat



Figure 3. View of construction at Silangkitang Village Flat

3. Result and Discussion

The nonlinear static (pushover) analysis results reveal the comparative seismic performance of the shear wall and bracing systems. The capacity curves obtained for both systems illustrate their base shear–displacement relationships in the principal directions.

In the X-direction, the capacity curves, presented in Figure 4, show that the shear wall building reaches a target displacement of 66.84 mm with a base shear of 8512.78 kN, while the bracing building experiences a larger target displacement of 119.19 mm but with a higher base shear capacity of 9773.20 kN. Detailed incremental results of the pushover steps for both structural systems are provided in Tables 2 and 3.

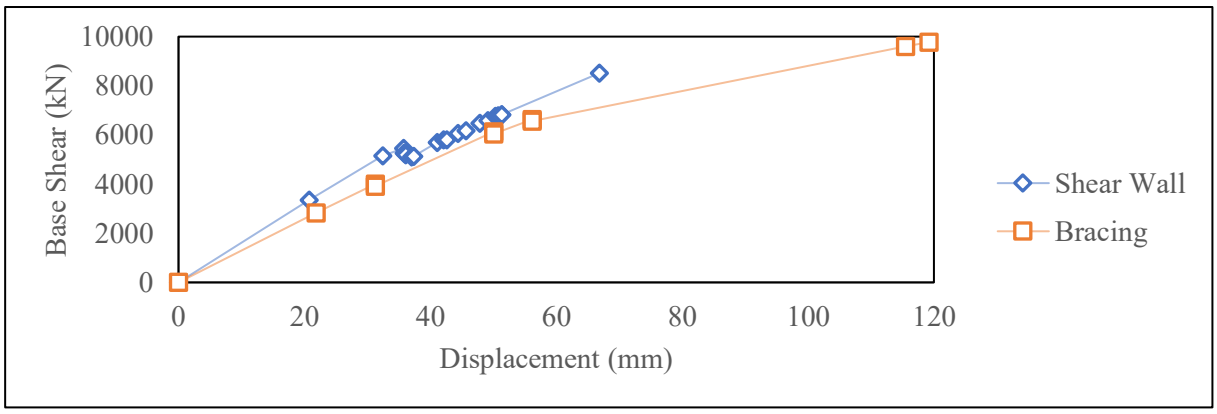


Figure 4. Comparison of capacity curves in buildings in X direction

Table 2. The capacity curve in the shear wall building in the X direction

Step	Disp. (mm)	Base Shear (kN)	Plastic Hinge States (A–B / B–C / C–D / D–E / >E)	Performance Level Dist. (A–IO / IO–LS / LS–CP / >CP)	Total
0	0	0	822 / 0 / 0 / 0 / 0	822 / 0 / 0 / 0	822
1	20.705	3354.406	818 / 4 / 0 / 0 / 0	822 / 0 / 0 / 0	822
2	32.453	5151.91	818 / 4 / 0 / 0 / 0	821 / 0 / 0 / 1	822
3	35.695	5452.647	818 / 4 / 0 / 0 / 0	821 / 0 / 0 / 1	822
4	35.817	5260.822	817 / 4 / 1 / 0 / 0	821 / 0 / 0 / 1	822
5	35.964	5244.261	817 / 3 / 2 / 0 / 0	821 / 0 / 0 / 1	822
6	36.074	5190.337	817 / 3 / 2 / 0 / 0	821 / 0 / 0 / 1	822
7	37.044	5108.381	816 / 4 / 1 / 1 / 0	821 / 0 / 0 / 1	822
8	37.382	5124.316	816 / 4 / 0 / 2 / 0	821 / 0 / 0 / 1	822
9	41.074	5692.237	812 / 8 / 0 / 2 / 0	821 / 0 / 0 / 1	822
10	42.127	5793.178	809 / 11 / 0 / 2 / 0	821 / 0 / 0 / 1	822
11	42.631	5793.526	808 / 12 / 0 / 2 / 0	821 / 0 / 0 / 1	822
12	44.41	6061.135	794 / 26 / 0 / 2 / 0	821 / 0 / 0 / 1	822
13	45.635	6167.789	792 / 28 / 0 / 2 / 0	821 / 0 / 0 / 1	822
14	47.861	6469.273	771 / 49 / 0 / 2 / 0	821 / 0 / 0 / 1	822
15	49.13	6584.753	757 / 63 / 0 / 2 / 0	821 / 0 / 0 / 1	822
16	50.311	6748.125	749 / 71 / 0 / 2 / 0	821 / 0 / 0 / 1	822
17	50.718	6775.178	739 / 81 / 0 / 1 / 1	821 / 0 / 0 / 1	822
18	50.77	6751.998	739 / 81 / 0 / 1 / 1	821 / 0 / 0 / 1	822
19	50.873	6765.933	739 / 81 / 0 / 1 / 1	821 / 0 / 0 / 1	822
20	50.879	6766.805	738 / 82 / 0 / 1 / 1	821 / 0 / 0 / 1	822
21	51.307	6832.863	728 / 92 / 0 / 1 / 1	821 / 0 / 0 / 1	822
22	51.313	6833.783	728 / 92 / 0 / 1 / 1	821 / 0 / 0 / 1	822
23	66.84	8512.779	587 / 233 / 0 / 0 / 2	819 / 2 / 0 / 1	822

Table 3. The capacity curve in the bracing building in the X direction

Step	Disp. (mm)	Base Shear (kN)	Plastic Hinge States (A–B / B–C / C–D / D–E / >E)	Performance Level Dist. (A–IO / IO–LS / LS–CP / >CP)	Total
0	0	0	862 / 0 / 0 / 0 / 0	862 / 0 / 0 / 0	862
1	21.798	2828.474	861 / 1 / 0 / 0 / 0	862 / 0 / 0 / 0	862
2	31.25	4008.724	858 / 3 / 1 / 0 / 0	857 / 5 / 0 / 0	862
3	31.256	3904.701	858 / 2 / 0 / 2 / 0	856 / 6 / 0 / 0	862
4	50.033	6121.61	784 / 75 / 1 / 2 / 0	854 / 4 / 4 / 0	862
5	50.039	6043.981	782 / 77 / 0 / 3 / 0	853 / 5 / 4 / 0	862
6	56.162	6634.722	725 / 132 / 1 / 3 / 1	853 / 5 / 3 / 1	862
7	56.168	6557.856	724 / 133 / 0 / 4 / 1	852 / 6 / 3 / 1	862
8	115.484	9610.009	534 / 317 / 3 / 4 / 4	800 / 51 / 3 / 8	862
9	119.191	9773.201	532 / 319 / 2 / 5 / 4	795 / 53 / 6 / 8	862

Similarly, in the Y-direction, as illustrated in Figure 5, the shear wall building achieves a target displacement of 166 mm with a base shear capacity of 13,228.69 kN, while the bracing building shows

a slightly greater displacement of 173 mm but a lower base shear capacity of 8210.53 kN. The full results of the pushover increments in this direction are presented in Tables 4 and 5.

These capacity curves indicate that the shear wall system generally provides greater lateral stiffness, as reflected in the lower displacement demands at comparable or higher base shear levels. Conversely, the bracing system exhibits more deformability (higher displacement) but reduced strength in some directions, particularly in the Y-axis. This behavior aligns with fundamental mechanics: bracing redistributes lateral loads into axial forces within the frame, increasing flexibility but not necessarily enhancing overall structural stiffness, whereas shear walls act as rigid vertical elements that resist both shear and moment, improving lateral rigidity.

Story shear distributions are summarized in Table 6 and visualized in Figure 6, showing that the bracing system generates slightly higher roof-level shear in the X-direction (1396.62 kN vs. 1216.13 kN) but lower in the Y-direction (178.13 kN vs. 254.39 kN) compared to the shear wall system. Similarly, Table 7 and Figure 7 present the story displacements, confirming that bracing buildings exhibit higher roof displacements in both directions, reflecting reduced lateral stiffness and higher flexibility.

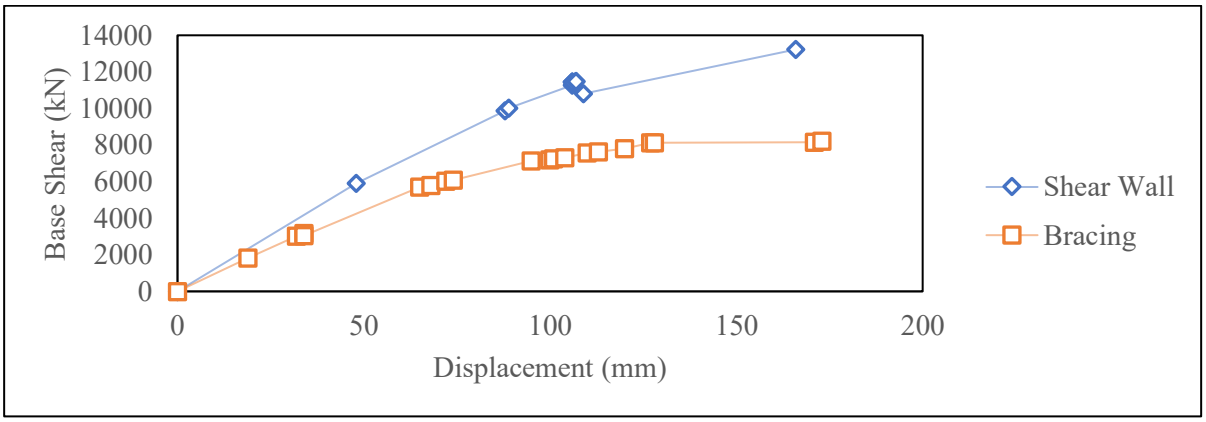


Figure 5. Comparison of capacity curves in buildings in Y direction

Table 4. The capacity curve in the shear wall building in the Y direction

Step	Disp. (mm)	Base Shear (kN)	Plastic Hinge States (A–B / B–C / C–D / D–E / >E)	Performance Level Dist. (A–IO / IO–LS / LS–CP / >CP)	Total
0	0	0	822 / 0 / 0 / 0 / 0	822 / 0 / 0 / 0	822
1	48	5905.706	814 / 8 / 0 / 0 / 0	822 / 0 / 0 / 0	822
2	88	9873.384	797 / 23 / 2 / 0 / 0	818 / 4 / 0 / 0	822
3	89	10009.585	795 / 25 / 2 / 0 / 0	818 / 4 / 0 / 0	822
4	106	11273.226	784 / 36 / 2 / 0 / 0	816 / 4 / 2 / 0	822
5	106	11461.31	779 / 41 / 2 / 0 / 0	816 / 4 / 2 / 0	822
6	106	11464.745	779 / 41 / 2 / 0 / 0	816 / 4 / 2 / 0	822
7	107	11467.911	779 / 41 / 2 / 0 / 0	816 / 4 / 2 / 0	822
8	107	11470.796	779 / 41 / 2 / 0 / 0	816 / 4 / 2 / 0	822
9	109	10799.208	779 / 41 / 2 / 0 / 0	816 / 4 / 2 / 0	822
10	166	13228.694	719 / 101 / 2 / 0 / 0	812 / 6 / 4 / 0	822

Table 5. The capacity curve in the bracing building in the Y direction

Step	Disp. (mm)	Base Shear (kN)	Plastic Hinge States (A–B / B–C / C–D / D–E / >E)	Performance Level Dist. (A–IO / IO–LS / LS–CP / >CP)	Total

0	0	0	862 / 0 / 0 / 0 / 0	862 / 0 / 0 / 0	862
1	19	1823.563	858 / 4 / 0 / 0 / 0	862 / 0 / 0 / 0	862
2	32	3030.421	852 / 8 / 2 / 0 / 0	862 / 0 / 0 / 0	862
3	34	3171.981	850 / 8 / 2 / 2 / 0	860 / 2 / 0 / 0	862
4	34	3041.803	850 / 8 / 0 / 4 / 0	858 / 4 / 0 / 0	862
5	65	5715.43	833 / 25 / 0 / 4 / 0	856 / 4 / 0 / 2	862
6	68	5805.767	830 / 28 / 0 / 4 / 0	856 / 4 / 0 / 2	862
7	72	6020.107	823 / 35 / 0 / 4 / 0	855 / 5 / 0 / 2	862
8	74	6073.874	820 / 38 / 0 / 4 / 0	855 / 5 / 0 / 2	862
9	95	7141.969	789 / 69 / 0 / 4 / 0	853 / 7 / 0 / 2	862
10	100	7206.261	784 / 74 / 0 / 4 / 0	853 / 7 / 0 / 2	862
11	101	7262.754	777 / 81 / 0 / 4 / 0	853 / 7 / 0 / 2	862
12	104	7320.591	772 / 86 / 0 / 4 / 0	852 / 7 / 0 / 3	862
13	110	7576.541	742 / 116 / 0 / 4 / 0	852 / 6 / 1 / 3	862
14	113	7619.639	739 / 119 / 0 / 4 / 0	852 / 6 / 1 / 3	862
15	120	7812.164	727 / 131 / 0 / 4 / 0	850 / 8 / 1 / 3	862
16	127	8115.354	717 / 141 / 0 / 4 / 0	839 / 13 / 6 / 4	862
17	128	8115.859	717 / 141 / 0 / 4 / 0	839 / 13 / 6 / 4	862
18	171	8151.863	715 / 142 / 0 / 4 / 1	839 / 13 / 5 / 5	862
19	173	8210.534	709 / 148 / 0 / 4 / 1	838 / 14 / 5 / 5	862

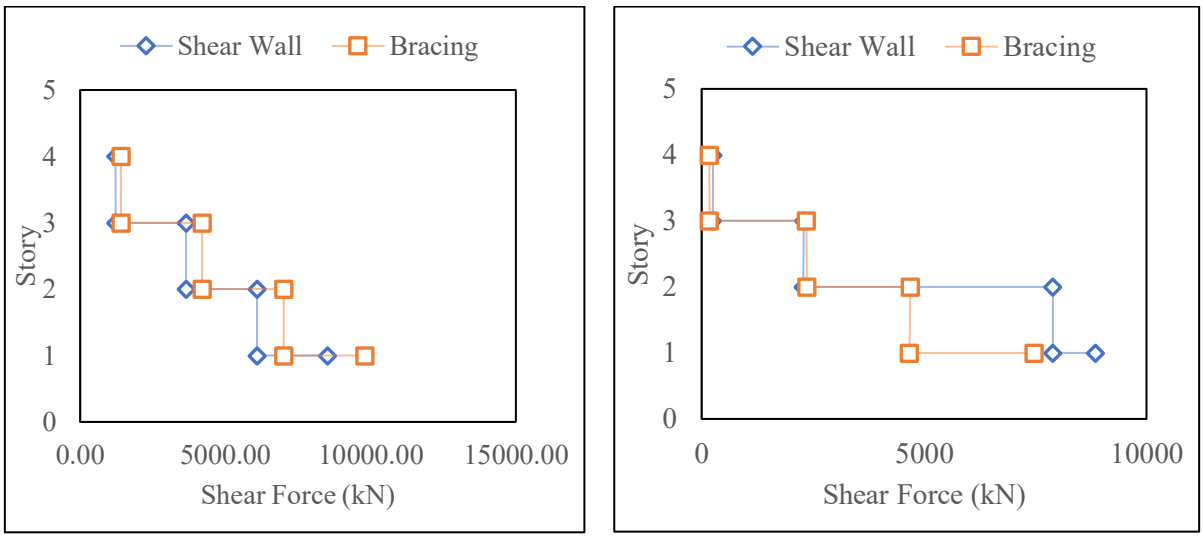


Figure 6. Comparison of story shear in buildings in X direction (left) and Y direction (Right)

Table 6. Story shear in shear wall and bracing building in X and Y direction

Structure Type	**Shear Wall (mm)**		**Bracing (mm)**	
Story	**X Direction**	**Y Direction**	**X Direction**	**Y Direction**
Roof	1,216.13	254.3868	1,396.62	178.1259
	1,216.23	250.456	1,399.57	177.5614
Roof Deck	3,648.51	2,297.44	4,194.49	2,350.04
	3,648.59	2,282.60	4,199.64	2,365.10
Story 3	6,080.74	7,895.54	6,998.91	4,689.64
	6,080.61	7,893.70	7,005.01	4,672.28
Story 2	8,511.49	8,856.16	9,804.59	7,478.36
	8,512.35	8,846.21	9,809.56	7,475.27

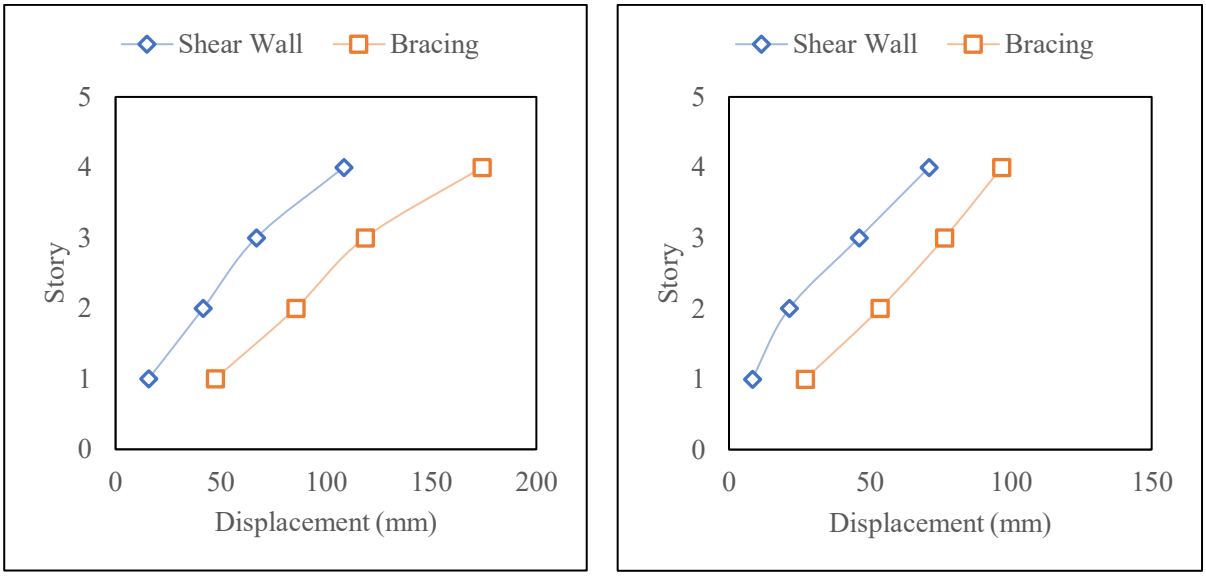


Figure 7. Comparison of story displacement in buildings in X direction (left) and Y direction (Right)

Table 7. Story displacement in shear wall and bracing building in X and Y direction

Structure Type	**Shear Wall (mm)**		**Bracing (mm)**	
Story	**X Direction**	**Y Direction**	**X Direction**	**Y Direction**
Roof	108.387	70.98	174.188	96.759
	−0.010	0.106	−0.010	−0.165
Roof Deck	66.838	46.109	118.524	76.397
	−0.003	0.009	−0.002	−0.223
Story 3	41.636	21.332	85.515	53.519
	0.00015	0.012	0.00037	−0.154
Story 2	15.672	8.213	47.313	27.052
	−0.00015	0.002	0.00012	−0.053

To quantify performance levels, maximum drift ratios were computed by dividing roof displacements by the building height, as summarized in Table 8. The results show that in the X-direction, both systems achieve the Immediate Occupancy (IO) level, while in the Y-direction, both satisfy the Damage Control (DC) level. These outcomes indicate compliance with performance-based design criteria such as ATC-40 and FEMA 440, which define acceptable drift limits for various seismic performance objectives.

Table 8. Calculation results of structural performance levels

Structure Type	**Direction**	**Total Displacement (mm)**	**Height (mm)**	**Maximum Drift**	**Performance Level**
Shear Wall Building	X	45.635	14600	0.0031	Immediate Occupancy
	Y	166	14600	0.0114	Damage Control
Bracing Building	X	119.191	14600	0.0081	Immediate Occupancy
	Y	173	14600	0.1185	Damage Control

A detailed interstory drift evaluation (Table 9 and Figure 8) further supports this conclusion, with both systems remaining within acceptable limits, indicating no soft-story mechanisms. However, the bracing system tends to produce slightly higher interstory drifts, particularly at upper levels, indicating more pronounced lateral flexibility under equivalent seismic demand.

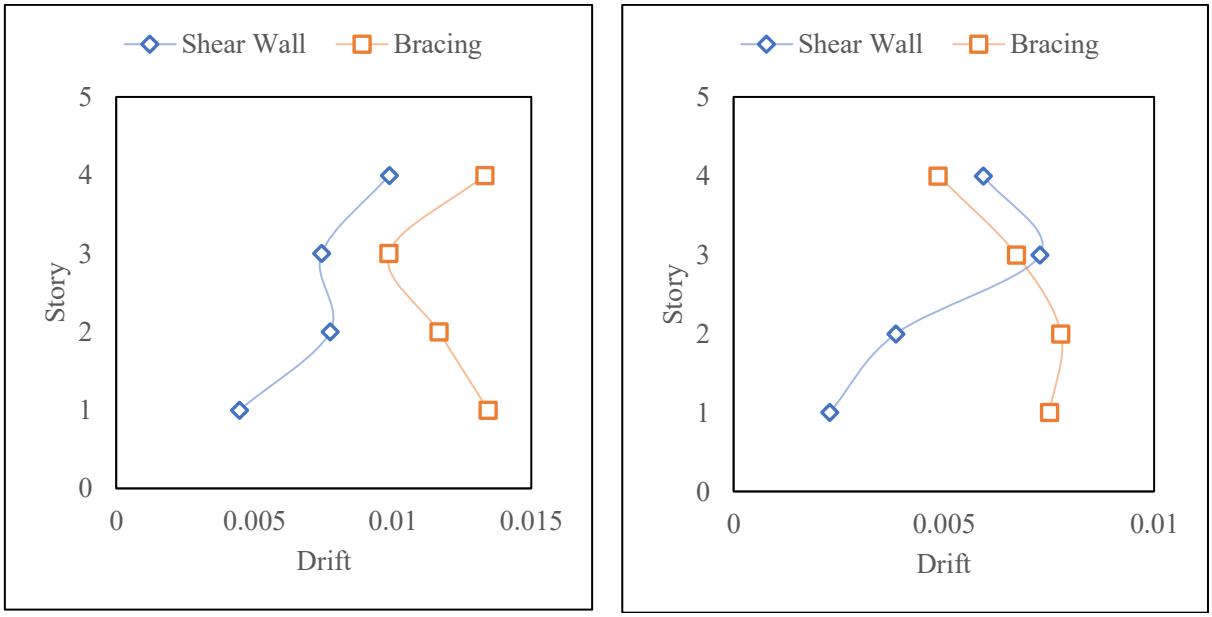


Figure 8. Comparison of story drift in buildings in X direction (left) and Y direction (Right)

Table 9. Calculation results of Story Drift

Story	**Shear Wall Building**		**Bracing Building**	
	Drift X	**Drift Y**	**Drift X**	**Drift Y**
Roof	0.00987	0.00594	0.01332	0.005
Roof Deck	0.00742	0.00729	0.00985	0.00673
Story 3	0.00773	0.00386	0.01166	0.00779
Story 2	0.00446	0.00229	0.01344	0.00751

The formation and distribution of plastic hinges provide additional insight into ductility demands. As shown in Figure 9 and Figure 10, the shear wall building in the X-direction forms 822 plastic hinges, with only one hinge exceeding the Collapse Prevention (CP) limit (>CP). In contrast, the bracing building develops 862 plastic hinges, with eight hinges exceeding the CP threshold, indicating a higher probability of localized failure under extreme seismic events. A similar trend is observed in the Y-direction, where the shear wall system exhibits fewer critical hinges compared to the bracing system.

The analysis indicates that both structural systems comply with established seismic performance criteria, as the computed maximum drift ratios remain within the ATC-40 and FEMA 440 limits for Immediate Occupancy (IO) and Damage Control (DC) levels. This confirms that both designs successfully achieve the intended seismic performance objectives. However, the bracing system exhibits increased displacement due to its relatively lower lateral stiffness compared to reinforced concrete shear walls. While bracing effectively transfers lateral forces as axial forces within the frame, it does not contribute to the building's overall rigidity to the same extent as shear walls. As a result, larger deformations occur, and the effective lateral load-resisting capacity (base shear) may decrease in certain directions due to reduced moment resistance and higher flexibility.

In contrast, shear walls provide continuous vertical elements with superior in-plane stiffness and strength, enabling them to resist significant lateral forces with minimal deformation. The reduced displacement demands, fewer plastic hinges exceeding Collapse Prevention (CP) levels, and more favorable base shear distribution collectively demonstrate that shear wall systems deliver better global stability and a more predictable seismic response compared to bracing systems in this case study.

In summary, although both systems comply with the targeted seismic performance criteria, the shear wall system demonstrates superior seismic performance for the Silangkitang Village Flats by providing improved lateral stiffness, reduced displacement demands, and enhanced structural reliability under pushover analysis.

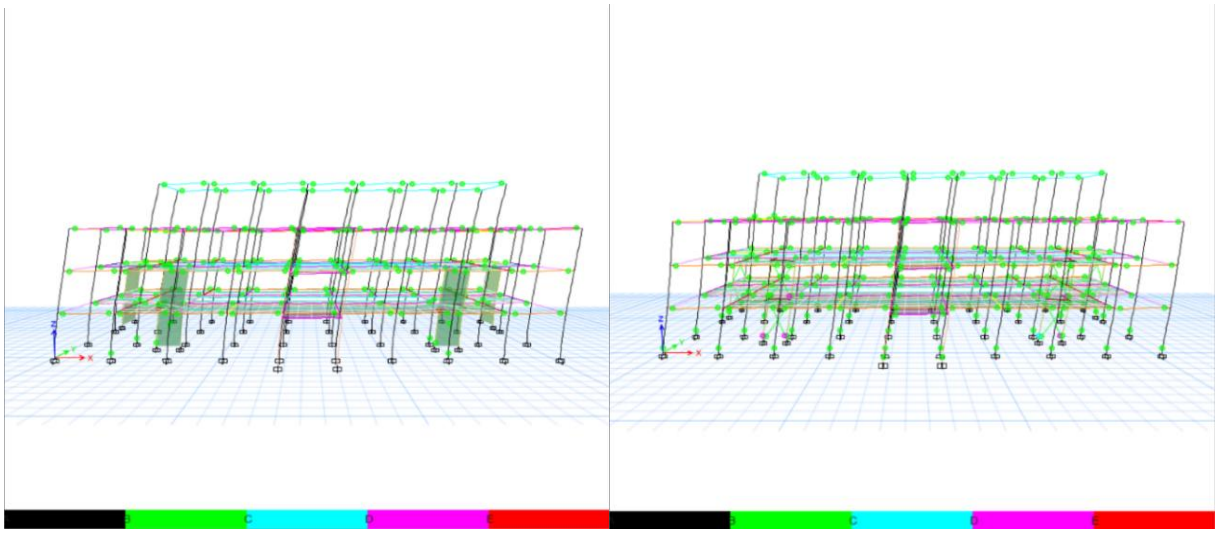


Figure 9. Plastic hinges in shear wall buildings (left) and bracing buildings (right) in the X direction

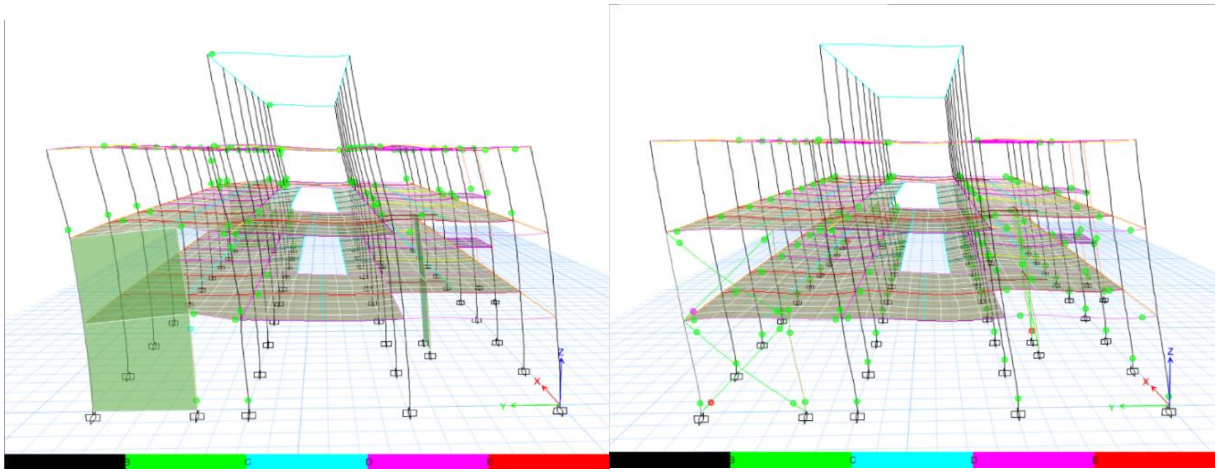


Figure 10. Plastic hinges in shear wall buildings (left) and bracing buildings (right) in the Y direction

4. Conclusion

Based on the nonlinear static (pushover) analysis of the Silangkitang Village Flats, Sipoholon District, North Tapanuli Regency, it can be concluded that both the shear wall and bracing structural systems are capable of providing adequate resistance against earthquake-induced lateral loads, achieving similar overall seismic performance levels in accordance with the specified design criteria. However, the shear wall building demonstrated slightly superior structural performance compared to the bracing building. This superiority is reflected in its lower maximum inter-story drift ratios (0.0031 in the X-direction and 0.0114 in the Y-direction) compared with the bracing building (0.0081 in the X-direction and 0.1185 in the Y-direction), indicating reduced lateral deformation under seismic excitation. Additionally, the shear wall building experienced smaller total roof displacements, recorded at 45.635 mm and 166.000 mm in the X and Y directions, respectively, compared to 119.191 mm and 173.000 mm for the bracing system, signifying greater lateral stiffness.

The distribution of plastic hinges in the shear wall building was concentrated at predictable locations, particularly at the base of the walls, ensuring controlled inelastic behavior and enhancing post-earthquake reparability. In contrast, the bracing system exhibited a wider spread of yielding, potentially increasing non-structural damage risks. Overall, these findings indicate that for mid-rise residential buildings constructed under similar seismic and geotechnical conditions, reinforced concrete shear walls provide a more efficient lateral load-resisting mechanism than steel bracing frames by offering improved stiffness, better drift control, and more predictable inelastic behavior while maintaining compliance with targeted seismic performance objectives.

References

[1] N. Suprapto and I. A. Rizki, "Evaluation of geohazards research in the world and Pacific region: A comparative bibliometric study," *The Iraqi Geological Journal*, pp. 143-161, 2024.

[2] P. Lemenkova, "Java and sumatra segments of the sunda trench: Geomorphology and geophysical settings analysed and visualized by GMT," *Гласник Српског географског друштва*, vol. 100, no. 2, pp. 1-23, 2020.

[3] S. S. Shareef, "Earthquake consideration in architectural design: Guidelines for architects," *Sustainability*, vol. 15, no. 18, p. 13760, 2023.

[4] M. Shahjalal, A. K. M. Yahia, A. S. M. Morshed, and N. I. Tanha, "Earthquake-resistant building design: Innovations and challenges," *Global Mainstream Journal of Innovation, Engineering & Emerging Technology*, vol. 3, no. 4, pp. 101-119, 2024.

[5] I. A. David, K. Mohammed, N. Muazu, and M. S. Nadro, "Seismic behaviour of high-rise buildings equipped with fluid viscous dampers: A review," *ARID Zone Journal of Engineering, Technology and Environment*, vol. 21, no. 2, pp. 460-475, 2025.

[6] F. O. Okeke, C. A. Okeke, and N. N. Mbamalu, "Building architectural design and fundamental loading considerations," *Nnamdi Azikiwe Univ. Ser. III Sustain. Dev., Nnamdi Azikiwe University, Awka*, pp. 79-89, 2023.

[7] M. M. I. Mazhar, "Structural design and analysis of a 20-story mixed-use high-rise residential and commercial building in Dhaka: Seismic and wind load considerations," *Global Mainstream Journal of Innovation, Engineering & Emerging Technology*, vol. 3, no. 4, pp. 10-62304, 2024.

[8] M. A. Bezabeh, G. T. Bitsuamlak, and S. Tesfamariam, "Performance-based wind design of tall buildings: Concepts, frameworks, and opportunities," *Wind Struct*, vol. 31, no. 2, pp. 103-142, 2020.

[9] E. J. Sulonteh and A. Mahajan, "Seismic performance of high-rise buildings with advanced lateral load resisting systems subjected to wind and earthquake loads," *Asian Journal of Civil Engineering*, vol. 25, no. 7, pp. 5377-5391, 2024.

[10] A. Goli, M. Alaghmandan, and F. Barazandeh, "Parametric structural topology optimization of high-rise buildings considering wind and gravity loads," *Journal of Architectural Engineering*, vol. 27, no. 4, p. 04021038, 2021.

[11] S. A. Memon, M. Zain, D. Zhang, S. K. U. Rehman, M. Usman, and D. Lee, "Emerging trends in the growth of structural systems for tall buildings," *Journal of Structural Integrity and Maintenance*, vol. 5, no. 3, pp. 155-170, 2020.

[12] C. Qiu, L. Cheng, and X. Du, "Seismic analysis and design of a resilient steel frame with multiple lateral force–resisting systems," *Journal of Structural Engineering*, vol. 150, no. 7, p. 04024064, 2024.

[13] C. Wang, P. Tian, and T. M. Chan, "Seismic behavior of modular buildings with reinforced concrete (RC) structural walls as seismic force resisting system," *Engineering Structures*, vol. 315, p. 118378, 2024.

[14] M. Khademi, M. Tehranizadeh, and A. Shirkhani, "Case studies on the seismic resilience of reinforced concrete shear wall buildings and steel dual concentrically braced buildings," in *Structures*, vol. 58, p. 105596, Elsevier, Dec. 2023.

[15] J. Li, N. I. Fomin, S. Xiao, K. Yang, S. Zhao, and H. Yang, "Seismic enhancement techniques for reinforced concrete frame buildings: A contemporary review," *Buildings*, vol. 15, no. 6, p. 984, 2025.

[16] J. Kent, C. Zhong, and C. Christopoulos, "Steel flexure and shear yielding base-mechanism for enhanced seismic resilience of RC core wall high-rise structures," *Earthquake Spectra*, vol. 39, no. 1, pp. 148-170, 2023.

[17] A. Al Samouly, "High-performance steel-timber composite rocking shear-wall system for the next generation of tall mass timber buildings: seismic design for system acceptability," Ph.D. dissertation, University of British Columbia, 2023.

[18] H. M. Afefy, "Seismic retrofitting of reinforced-concrete coupled shear walls: A review," *Practice Periodical on Structural Design and Construction*, vol. 25, no. 3, p. 03120001, 2020.

[19] M. Shakeel, R. Azam, M. R. Riaz, and A. Shihata, "Design optimization of reinforced concrete cantilever retaining walls: A state-of-the-art review," *Advances in Civil Engineering*, vol. 2022, no. 1, p. 4760175, 2022.

[20] K. F. Ozturk, T. Cakir, and O. Araz, "Influences of wall configurations on earthquake behavior of cantilever retaining walls considering soil-structure interaction effects," *Journal of Earthquake and Tsunami*, vol. 17, no. 1, p. 2250021, 2023.

[21] A. Abbaszadeh and O. Chaallal, "Enhancing resilience and self-centering of existing RC coupled and single shear walls using EB-FRP: State-of-the-art review and research needs," *Journal of Composites Science*, vol. 6, no. 10, p. 301, 2022.

[22] C. A. Rodríguez, Á. M. Rodríguez Pérez, R. Lopez, and J. J. Caparrós Mancera, "Comparative analysis and evaluation of seismic response in structures: Perspectives from non-linear dynamic analysis to pushover analysis," *Applied Sciences*, vol. 14, no. 6, p. 2504, 2024.

[23] W. Carofilis, D. Perrone, G. J. O'Reilly, R. Monteiro, and A. Filiatrault, "Seismic retrofit of existing school buildings in Italy: Performance evaluation and loss estimation," *Engineering Structures*, vol. 225, p. 111243, 2020.

[24] S. Kumar and S. A. R. S. Hasibuan, "Kajian analisis struktur gedung 2D dengan ketidakberaturan vertikal menggunakan metode nonlinear pushover," *Sultra Civil Engineering Journal (SCiEJ)*, vol. 6, no. 1, pp. 424-436, 2025.

[25] S. A. R. S. Hasibuan, H. Prayuda, A. Alisibramulisi, S. H. Adnan, and T. A. R. Hussin, "Enhancing seismic resilience: The role of drop panels in building structures using pushover analysis," 2025.

[26] P. S. Hutabalian and S. A. R. S. Hasibuan, "Analisis struktur gedung 2D dengan ketidakberaturan vertikal menggunakan metode nonlinear pushover," *Jurnal Teknik Sipil dan Teknologi Konstruksi*, vol. 11, no. 1, 2025.

[27] B. N. Sitohang and S. A. R. S. Hasibuan, "Evaluasi kinerja seismik struktur gedung apartemen Princeton Boutique Living Medan," *Jurnal Teslink: Teknik Sipil dan Lingkungan*, vol. 5, no. 2, pp. 117-126, 2023.

[28] A. Abd-Elhamed, S. Mahmoud, and K. S. Alotaibi, "Nonlinear analysis of reinforced concrete buildings with different heights and floor systems," *Scientific Reports*, vol. 13, no. 1, p. 14949, 2023.

[29] H. Chaudhary and A. K. Tiwary, "Seismic analysis of steel bracing on composite structure by pushover analysis," *Journal of The Institution of Engineers (India): Series A*, vol. 104, no. 4, pp. 927-941, 2023.

[30] K. Javaid and N. Verma, "Seismic performance of irregular composite buildings: A comparative study of the effectiveness of buckling restrained braces and viscous dampers," *Materials Today: Proceedings*, 2023.

[31] A. Deng, "Database task processing optimization based on performance evaluation and machine learning algorithm," *Soft Computing-A Fusion of Foundations, Methodologies & Applications*, vol. 27, no. 10, 2023.

[32] M. Amjad, I. Ahmad, M. Ahmad, P. Wróblewski, P. Kamiński, and U. Amjad, "Prediction of pile bearing capacity using XGBoost algorithm: Modeling and performance evaluation," *Applied Sciences*, vol. 12, no. 4, p. 2126, 2022.

[33] M. S. Aslanpour, S. S. Gill, and A. N. Toosi, "Performance evaluation metrics for cloud, fog and edge computing: A review, taxonomy, benchmarks and standards for future research," *Internet of Things*, vol. 12, p. 100273, 2020.

[34] S. Jyothirmayee, B. D. K. Reddy, M. Rakesh, S. Pooja, T. Neha, and G. K. Naik, "A comparative study on design of commercial building using Etabs and Staad Pro," in *Journal of Physics: Conference Series*, vol. 2779, no. 1, p. 012035, IOP Publishing, June 2024.

[35] B. J. Nestor, M. S. Alfonso, and G. H. C., "Design codes before 2000 and after 2015 applied to a structure in the highlands of Peru," in *2022 Congreso Internacional de Innovación y Tendencias en Ingeniería (CONIITI)*, pp. 1-6, IEEE, Oct. 2022.

[36] M. Abate, A. C. J. Evangelista, and V. W. Tam, "Advanced seismic analysis of a 44-story reinforced concrete building: A comparison of code-based and performance based design approaches," *Infrastructures*, vol. 10, no. 4, p. 93, 2025.

[37] B. Wibowo, S. Nisumanti, and F. Febryandi, "Analysis of building structure performance due to earthquake load with time history analysis method using ETABS (Extended Three-Dimensional Analysis of Building Systems) software (case study: the faculty of medicine building at IGM University)," in *E3S Web of Conferences*, vol. 464, p. 13001, EDP Sciences, 2023.